Direct Synthesis and Characterization of Titanium-Substituted Mesoporous Molecular Sieve SBA-15

Wen-Hua Zhang,[†] Jiqing Lu,[†] Bo Han,[†] Meijun Li,[†] Jinghai Xiu,[‡] Pinliang Ying,[†] and Can Li*[,†]

State Key Laboratory of Catalysis, Dalian Institute of Chemical Physics, Chinese Academy of Sciences, 457 Zhongshan Road, Dalian 116023, People's Republic of China, and State Key Laboratory of Fine Chemical Engineering, Dalian University of Technology, 158 Zhongshan Road, Dalian 116012, People's Republic of China

Received December 11, 2001. Revised Manuscript Received May 23, 2002

Ti-substituted mesoporous SBA-15 (Ti−SBA-15) materials have been synthesized by using a new approach in which the hydrolysis of the silicon precursor (tetramethoxysilane, TMOS) is accelerated by fluoride. These materials were characterized by powder X-ray diffraction patterns (XRD), X-ray fluorescence spectroscopy (XRF), N_2 sorption isotherms, diffuse-reflectance UV−visible (UV−vis) and UV−Raman spectroscopy, ^{29}Si MAS NMR, and the catalytic epoxidation reaction of styrene. Experiments show that Ti−SBA-15 samples of high quality can be obtained under the following conditions: F/Si ≥ 0.03 (molar ratio), pH ≤ 1.0, aging temperature ≤ 80 °C, and Ti/Si ≤ 0.01. It was found that the hydrolysis rate of TMOS was remarkably accelerated by fluoride, which was suggested to play the main role in the formation of Ti−SBA-15 materials of high quality. There is no stoichiometric incorporation of Ti, and the Ti contents that are obtained are quite low in the case of the approach that is proposed. The calcined Ti−SBA-15 materials show highly catalytic activity in the epoxidation of styrene.

Introduction

Titanium-substituted zeolites have received great attention in past decades because of their excellent catalytic properties in selective oxidation reactions when using aqueous hydrogen peroxide as the oxidant.[1,21,2] However, most of them are microporous solids, and their applications are restricted to relatively small molecules, owing to the pore-size limitation.[3] In 1992, researchers at Mobil Corporation reported a series of ordered mesoporous silicates that were designated M41S,[4] which were synthesized through the self-assembly of surfactants and inorganic species. Since then, much effort has been dedicated to studying the synthesis[5,6] and applications of ordered mesoporous materials.[5,7] The most extensively studied member of the ordered mesoporous materials has been MCM-41, which possesses a large specific surface area, a hexagonal array, and uniform mesopore channels.[4] These properties make MCM-41-related materials among the best candidates for a wide range of applications in catalysis and sorption for large organic molecules, chromatographic separation, and host−guest chemistry.[8] However, MCM-41 materials are not as active in catalyzing bulky molecules as would be desired.[9] Hence, many elements such as B, Al, Ga, Mn, V, Nb, Cr, Sn, Zr, and Ti have been incorporated into the siliceous frameworks of MCM-related materials to create catalytic active sites.[5] These metal-substituted materials are usually prepared under basic conditions. However, reports on the successful preparation of metal-

* Corresponding author. E-mail: canli@ms.dicp.ac.cn. Fax: 86-411-4694447.
[†] Dalian Institute of Chemical Physics.
[‡] Dalian University of Technology.

(1) For recent reviews, see (a) Hölderich, W.; Hesse, M.; Näumann, M. *Angew. Chem., Int. Ed. Engl.* **1988**, *27*, 226. (b) Notari, B. *Adv. Catal.* **1996**, *41*, 253. (c) Arends, I. W. C. E.; Sheldon, R. A.; Wallau, M.; Schuchardt, U. *Angew. Chem., Int. Ed. Engl.* **1997**, *36*, 1144.

(2) (a) Clerici, M. G.; Bellussi, G.; Romano, U. *J. Catal.* **1991**, *129*, 159. (b) Khouw, C. B.; Davis, M. E. *J. Catal.* **1995**, *151*, 77. (c) Tuel, A.; Buskens, P.; Jacobs, P. A. *Appl. Catal.* **1993**, *102*, 69.

(3) Venuto, P. B. *Microporous Mater.* **1994**, *2*, 297.

(4) (a) Kresge, J. S.; Leonowicz, M. E.; Roth, W. J.; Vartuli, J. C.; Beck, J. S. *Nature (London)* **1992**, *359*, 710. (b) Beck, J. S.; Vartuli, J. C.; Roth, W. J.; Leonowicz, M. E.; Kresge, C. T.; Schmitt, K. D.; Chu, C. T.-W.; Olson, D. H.; Sheppard, E. W.; McCullen, S. C.; Higgins, J. B.; Schlenker, J. L. *J. Am. Chem. Soc.* **1992**, *114*, 10834.

(5) For recent reviews, see (a) Corma, A. *Chem. Rev.* **1997**, *97*, 2373. (b) Raman, N. K.; Anderson, M. T.; Brinker, C. J. *Chem. Mater.* **1996**, *8*, 1682. (c) Moller, K.; Bein, T. *Chem. Mater.* **1998**, *10*, 2950. (d) Ying, Y. J.; Mehnert, C. P.; Wong, M. S. *Angew. Chem., Int. Ed. Engl.* **1999**, *38*, 56.

(6) (a) Huo, Q.; Margolese, D. I.; Ciesla, U.; Feng, P.; Gier, T. E.; Sieger, P.; Leon, R.; Petroff, P. M.; Firouzi, A.; Schuth, F.; Stucky, G. D. *Nature (London)* **1994**, *368*, 317. (b) Tanev, P. T.; Pinnavaia, T. J. *Science (Washington, D.C.)* **1995**, *267*, 865. (c) Bagshaw, S. A.; Prouzet, E.; Pinnavaia, T. J. *Science (Washington, D.C.)* **1995**, *269*, 1242. (d) Inagaki, S.; Guan, S.; Fukushima, Y.; Ohsuna, T.; Terasaki, O. *J. Am. Chem. Soc.* **1999**, *121*, 9611.

(7) For examples, see (a) Feng, X.; Fryxell, G. E.; Wang, L.-Q.; Kim, A. Y.; Liu, J.; Kemner, K. M. *Science (Washington, D.C.)* **1997**, *267*, 923. (b) Zhou, W.; Thomas, J. M.; Shephard, D. S.; Johnson, B. F. G.; Ozkaya, D.; Maschmeyer, T.; Bell, R. G.; Ge, Q. *Science (Washington, D.C.)* **1998**, *280*, 705. (c) Ganschow, M.; Wark, M.; Wöhrle, D.; Schulz-Ekloff, G. *Angew. Chem., Int. Ed.* **2000**, *39*, 161. (d) Zhang, W.-H.; Shi, J.-L.; Wang, L.-Z.; Yan, D.-S. *Chem. Mater.* **2000**, *12*, 1408. (e) Zhang, W.-H.; Shi, J.-L.; Chen, H.-R.; Hua, Z.-L.; Yan, D.-S. *Chem. Mater.* **2001**, *13*, 648.

(8) Chenite, A.; Page, Y. L.; Sayari, A. *Chem. Mater.* **1995**, *7*, 1015.

(9) Corma, A.; Grand, M. S.; Gonzalez-Alfrao, V.; Orichilles, A. V. *J. Catal.* **1996**, *159*, 375.

10.1021/cm011686c CCC: $22.00
Published on Web 06/27/2002

doped mesoporous materials under acidic conditions are very few,[10] which might be due to the easy dissociation of metal−O−Si bonds under acidic, hydrothermal conditions. Metal ions are generally in an isolated state in acidic solution, whereas they easily precipitate from solution to form metal oxides in basic solution. Therefore, metal ions should be more highly dispersed in the metal-substituted mesoporous materials prepared under acidic conditions than in those prepared under basic conditions.

Researchers in Corma's[11] and in Pinnavaia's group[12] independently reported the preparation and catalytic activity of Ti-containing mesoporous materials in 1994 by using CTAB or dodecylamine as the structure-directing agent under basic conditions. Since then, much effort has been directed toward preparing Ti-substituted mesoporous materials to obtain an effective catalyst for large molecules[13] through similar methods. In 1996, Pinnavaia et al.[14] reported the synthesis of Ti-substituted MCM-41 under acidic conditions (pH $\approx$ 1.5). However, the poor hydrothermal stability of the MCM-41-related materials has restricted their potential applications. Thus, titanosilicate mesoporous materials with higher hydrothermal stability are highly desirable. Fortunately, a remarkable advance in the synthesis of ordered mesoporous materials was made by Zhao et al.[15] in 1998, who used triblock copolymer surfactants to template the formation of ordered large-pore mesoporous silica with different structures under strongly acidic conditions. This methodology was soon extended to the synthesis of ordered continuous mesoporous silica films,[16] fibers,[17] rods,[18] membranes,[19] spheres,[20] and monoliths.[21] Because of its easy synthesis, adjustable pore size, thick pore wall, and remarkable hydrothermal stability, the hexagonally ordered SBA-15 is currently the most prominent member of the family of triblock copolymer-templated materials. Many applications of SBA-15 materials in the fields of catalysis, sorption, and advanced material design can be envisioned. Specifically, SBA-15 materials functionalized by organosilanes have been utilized to sequestrate and release protein[22] and to remove heavy metals in pollutant solutions[23] and as chiral heterogeneous catalysts[24] and solid acids.[25] SBA-15 solids have also been used as matrixes to template the formation of metal nanowires[26] and mesoporous carbon molecule sieves.[27] After patterning with soft lithography, SBA-15 silica was found to be useful in waveguides and mirrorless lasers.[28]

Incorporation of transition-metal ions into the frameworks of molecular sieves is a common method used to introduce catalytic sites into zeolites[29] and mesoporous materials.[5] However, relatively little work has been done on the synthesis of the metal-substituted SBA-15 materials. Nevertheless, attempts have been made to prepare metal-containing SBA-15 via postsynthesis grafting reactions.[30] Yue et al.[31] have tried to incorporate aluminum directly into the frameworks of SBA-15 materials, but the result was many extraframework aluminum species. Xiao et al.[32] have used a complex method to synthesize metal-substituted SBA-15-like materials (metal = Al and Ti) in which the framework consists of nanocrystalline ZSM-5, which is much different from the other mesoporous materials that possess an amorphous framework. Newalkar et al.[33] have recently obtained Ti-containing SBA-15 materials using a microwave-assisted synthetic method. However, the challenge to prepare metal-substituted SBA-15 materials directly via the usual hydrothermal method remains. On the basis of synthetic conditions, this difficulty could be classified two ways. One is that SBA-15 materials have generally been synthesized under strongly acidic hydrothermal conditions that easily induce the dissociation of the Ti−O−Si bonds, if they have been formed. Another is the large difference in the hydrolysis rate between the titanium and silicon precursors, which are

(10) (a) Bagshaw, S. A.; Renzo, F. D.; Fajula, F. *Chem. Commun.* **1996**, 2209. (b) Raimondi, M. E.; Gianotti, E.; Marchese, L.; Martra, G.; Maschmeyer, T.; Seddon, J. M.; Coluccia, S. *J. Phys. Chem. B* **2000**, *104*, 7102. (c) Haskouri, J. E.; Cabrera, S.; Gutierrez, M.; Beltrán-Porter, A.; Beltrán-Porter, D.; Marcos, M. D.; Amorós, P. *Chem. Commun.* **2001**, 309. (d) Bagshaw, S. A.; Kemmitt, T.; Milestone, N. B. *Micro. Mesoporous Mater.* **1998**, *22*, 419.

(11) Corma, A.; Navarro, M. T.; Pariente, J. P. *J. Chem. Soc., Chem. Commun.* **1994**, 147.

(12) Tanev, P. T.; Chibwe, M.; Pinnavaia, T. J. *Nature (London)* **1994**, *368*, 321.

(13) For examples, see (a) Blasco, T.; Corma, A.; Navarro, M. T.; Pariente, J. P. *J. Catal.* **1995**, *156*, 65. (b) Alba, M. D.; Luan, Z.; Klinowski, J. *J. Phys. Chem.* **1996**, *100*, 2178. (c) Gontier, S.; Tuel, A. *J. Catal.* **1995**, *157*, 124.

(14) Zhang, W.; Fröba, M.; Wang, J.; Tanev, P. T.; Wong, J.; Pinnavaia, T. J. *J. Am. Chem. Soc.* **1996**, *118*, 9164.

(15) (a) Zhao, D.; Feng, J.; Huo, Q.; Melosh, N.; Fredrickson, G. H.; Chmelka, B. F.; Stucky, G. D. *Science (Washington, D.C.)* **1998**, *279*, 548. (b) Zhao, D.; Huo, Q.; Feng, J.; Chmelka, B. F.; Stucky, G. D. *J. Am. Chem. Soc.* **1998**, *120*, 6024.

(16) Zhao, D.; Yang, P.; Melosh, N.; Feng, J.; Chmelka, B. F.; Stucky, G. D. *Adv. Mater.* **1998**, *10*, 1380.

(17) Yang, P.; Zhao. D.; Chmelka, B. F.; Stucky, G. D. *Chem. Mater.* **1998**, *10*, 2033.

(18) Schmidt-Winkel, P.; Yang, P.; Margolese, D. I.; Chmelka, B. F.; Stucky, G. D. *Adv. Mater.* **1999**, *11*, 303.

(19) Zhao, D.; Yang, P.; Chmelka, B. F. Stucky, G. D. *Chem. Mater.* **1999**, *11*, 1174.

(20) Zhao, D.; Sun, J.; Li, Q.; Stucky, G. D. *Chem. Mater.* **2000**, *12*, 275.

(21) (a) Melosh, N. A.; Lipic, P.; Bates, F. S.; Wudl, F.; Stucky, G. D.; Fredrickson, G. H.; Chmelka, B. F. *Macromolecules* **1999**, *32*, 4332. (b) Feng, P.; Bu, X.; Stucky, G. D.; Pine, D. J. *J. Am. Chem. Soc.* **2000**, *122*, 994. (c) Melosh, N. A.; Davidson, P.; Chmelka, B. F. *J. Am. Chem. Soc.* **2000**, *122*, 823. (d) Feng, P.; Bu, X.; Pine, D. J. *Langmuir* **2000**, *16*, 5304.

(22) Han, Y.-J.; Stucky, G. D.; Butler, A. *J. Am. Chem. Soc.* **1999**, *121*, 9897.

(23) Liu, A. M.; Hidajat, K.; Kawi, S.; Zhao, D. Y. *Chem. Commun.* **2000**, 1145.

(24) Bae, S. J.; Kim, S.-W.; Hyeon, T.; Kim, B. M. *Chem. Commun.* **2000**, 31.

(25) (a) Margolese, D.; Melero, J. A.; Christiansen, S. C.; Chmelka, B. F.; Stucky, G. D. *Chem. Mater.* **2000**, *12*, 2448. (b) Corriu, R. J. P.; Datas, L.; Guari, Y.; Mehdi, A.; Reyé, C.; Thieuleux, C. *Chem. Commun.* **2001**, 763.

(26) (a) Han, Y.-J.; Kim, J. M.; Stucky, G. D. *Chem. Mater.* **2000**, *12*, 2068. (b) Ryoo, R.; Ko, C. H.; Kruk, M.; Antochshuk, V.; Jaroniec, M. *J. Phys. Chem. B* **2000**, *104*, 11465. (c) Huang, M. H.; Choudrey, A.; Yang, P. *Chem. Commun.* **2000**, 1063.

(27) (a) Jun, S.; Joo, S. H.; Ryoo, R.; Kruk, M.; Jaroniec, M.; Liu, Z.; Ohsuna, T.; Terasaki, O. *J. Am. Chem. Soc.* **2000**, *122*, 10712. (b) Shin, H. Y.; Ryoo, R.; Kruk, M.; Jaroniec, M. *Chem. Commun.* **2001**, 349.

(28) Yang, P.; Wirnsberger, G.; Huang, H. C.; Cordero, S. R.; McGehee, M. D.; Scott, B.; Deng, T.; Whitesides, G. M.; Chmelka, B. F.; Buratto, S. K.; Stucky, G. D. *Science (Washington, D.C.)* **2000**, *287*, 465.

(29) Szostak, R. *Molecular Sieves: Principles of Synthesis and Identification*; Van Nostrand Reinhold: New York, 1989; pp 211−238.

(30) (a) Luan, Z.; Hartmann, M.; Zhao, D.; Zhou, W.; Kevan, L. *Chem. Mater.* **1999**, *11*, 1621. (b) Luan, Z.; Maes, E. M.; van der Heide, P. A. W.; Zhao, D.; Czernuszewicz, R. S.; Kevan, L. *Chem. Mater.* **1999**, *11*, 3680. (c) Morey, M. S.; O'Brien, S.; Schwarz, S.; Stucky, G. D. *Chem. Mater.* **2000**, *12*, 898.

(31) Yue, Y.; Gédéon, A.; Bonardet, J.-L.; Melosh, N.; D'Espinose, J.-B.; Fraissard, J. *Chem. Commun.* **1999**, 1967.

(32) Han, Y.; Xiao, F.-S.; Wu, S.; Sun, Y.; Meng, X.; Li, D.; Lin, S.; Deng, F.; Ai, X. *J. Phys. Chem. B* **2001**, *105*, 7963.

(33) Newalkar, B. L.; Olanrewaju, J.; Komarneni, S. *Chem. Mater.* **2001**, *13*, 552.

usually alkoxides. The hydrolysis of titanium alkoxides is virtually instantaneous, whereas the hydrolysis of silicon precursors is much slower. Thus, two strategies could be applied to the preparation of Ti-substituted SBA-15 to satisfy the prerequisite of avoiding a strongly acidic hydrothermal treatment. One is to decrease the hydrolysis rate of the titanium precursors to match that of the silicon precursors; another is to accelerate the hydrolysis rate of the silicon precursors to match that of the titanium precursors. The former strategy has been utilized in preparing Ti-containing mesoporous materials[10a−c]; however, no studies using the latter have been reported. In the current study, we have used the latter strategy to explore an efficient approach to the direct synthesis of Ti-substituted SBA-15 (Ti−SBA-15) materials using fluoride to accelerate the hydrolysis rate of the silicon precursors.

Fluoride is a well-known catalyst for the hydrolysis and polymerization of silica species[34] and has been used in the synthesis of purely siliceous mesoporous materials under various conditions.[18,35] Kim et al.[36] have recently reported the synthesis of purely siliceous SBA-15 materials using TMOS as the silicon precursor in the presence of a small amount of fluoride over a wide pH range through hydrothermal treatment at 100 °C, and highly ordered SBA-15 materials have been obtained with pH ≤ 2.0. In this paper, we report a simple and efficient approach to the direct synthesis of Ti−SBA-15 materials using TMOS catalyzed by NH_4F. Experimental results show that Ti−SBA-15 materials of high quality can be synthesized in the presence of a certain amount of fluoride (F/Si ≈ 0.03−0.05) and at relatively low pH (≤1.0). The catalytic reaction of the epoxidation of styrene indicates that these materials are relatively highly active and selective.

Experimental Section

Synthesis. Ti−SBA-15 materials were prepared using TMOS and titanium isopropoxide (Acros) as silicon and titanium sources, respectively. Nonionic triblock copolymer surfactant $EO_{20}PO_{70}EO_{20}$ (P123, BASF) was used as the structure-directing agent. Concentrated HCl aqueous solution was used as the acid source. All reagents were used as received.

In a typical synthetic process, 2 g of P123 and a small amount of NH_4F were dissolved in 75 mL of HCl solution at pH 1.0. Then, ∼3.0−3.5 g of TMOS mixed with a calculated amount of titanium isopropoxide was added under vigorous stirring at ∼35−40 °C, and stirring was continued for about 20 h. The resultant mixture was then aged at 60 °C for 48 h without stirring. The samples were recovered, washed, and dried at 60 °C for at least 15 h. After calcination at 500 °C for 10 h in air, the mesoporous Ti−SBA-15 samples were finally obtained.

Characterization. XRD patterns were recorded on a Rigaku D/Max 3400 powder diffraction system using Cu Kα radiation (40 kV and 36 mA) over the range $0.5 \le 2\theta \le 6$. XRF spectra were obtained on a Philips MagiX spectrometer to determine the values of Ti/Si. The nitrogen sorption experiments were performed at 77 K on an ASAP 2000 system in static measurement mode. The samples were outgassed at 250 °C for 10 h before the measurement. The pore-size distribution curves were obtained from the analysis of the adsorption branch of the isotherm by the BJH (Barrett−Joyner−Halenda) method. Diffuse-reflectance UV−vis spectra were collected on a JASCO V-550 scanning spectrophotometer equipped with an integrating sphere from 190 to 600 nm. ^{29}Si MAS NMR spectra were recorded in 4-mm ZrO_2 rotors at 79.5 MHz on a Bruker DRX-400 spectrometer equipped with a magic angle spin probe, and qualitative analysis was performed. UV−Raman spectra were measured on a homemade UV−Raman spectrometer. The 244-nm line from a Coherent Innova 300 Fred was used as the excitation source. The power of the UV laser lines was less than 2.0 mW. The spectral resolution was estimated to be 4.0 cm^{-1}.

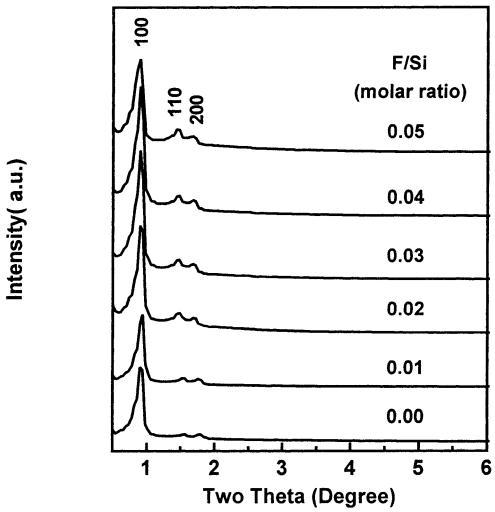

Figure 1. XRD patterns of Ti−SBA-15 samples synthesized at different fluoride contents.

The epoxidation of styrene was used as the test reaction. Typically, 15 mmol of styrene, 3 mmol of 30% H_2O_2, 10 mL of CH_3CN, and 0.3 g of catalyst were mixed in a 50-mL round-bottom flask and heated to 343 K under stirring for 3 h. The products were analyzed by a GC equipped with a capillary column (PEG-20M) and a FID detector. The conversion of styrene was calculated on the basis of the amounts of styrene and H_2O_2 that were used. The stoichiometric ratio of styrene/H_2O_2 is a unit, so the total conversion of styrene is defined as the point in which the amount of converted styrene is equal to the amount of H_2O_2 added.

Results and Discussion

A. Optimization of Fluoride Content. The content of fluoride is defined as the mole ratio of F/Si. Samples with different F contents, namely, 0.00, 0.01, 0.02, 0.03, 0.04, and 0.05, were synthesized to study the effect of fluoride on the quality of the resulting Ti−SBA-15 materials. The pH value of the HCl solution (before the P123 surfactant dissolved) was kept at 1.0, the aging temperature, at 60 °C, and the Ti /Si ratio, at 0.01. Figure 1 shows the XRD patterns of Ti−SBA-15 samples prepared with different fluoride contents. All samples show three diffraction peaks that can be indexed as the (100), (110), and (200) reflections, thus verifying that these samples are typical of hexagonal SBA-15 silica.[15] With the increase of F/Si from 0.00 to 0.03, the peak intensity increases appreciably, and the two small peaks, (110) and (200), become more clearly resolved, possibly because fluoride can improve the polymeriza-

(34) Brinker, C. J.; Scherer G. W. *Sol−Gel Science*; Academic Press: London, 1990; pp 97−234.

(35) (a) Prouzet, E.; Pinnavaia, T. J. *Angew. Chem., Int. Ed. Engl.* **1997**, *36*, 516. (b) Voegtlin, A. C.; Ruch, F.; Guth, J. L.; Patarin, J.; Huve, L. *Microporous Mater.* **1997**, *9*, 95. (c) Boissière, C.; Larbot, A.; Prouzet, E. *Chem. Mater.* **2000**, *12*, 1937. (d) Boissière, C.; Larbot, A.; van der Lee, A.; Kooyman, P. J.; Prouzet, E. *Chem. Mater.* **2000**, *12*, 2902.

(36) Kim. J. M.; Han, Y.-J.; Chmelka, B. F.; Stucky, G. D. *Chem. Commun.* **2000**, 2437.

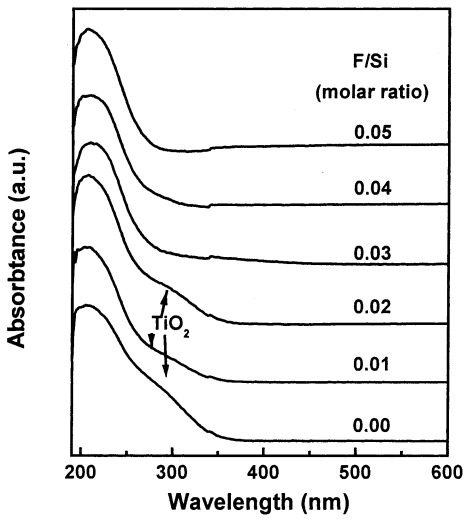

Figure 2. UV−vis absorption spectra of Ti−SBA-15 samples synthesized at different fluoride contents.

tion of the silanol groups.[34] However, some loss of peak intensity is observed when F/Si ≥ 0.03. This loss indicates that too high a fluoride content is detrimental to the quality of the SBA-15 materials. Similar studies have been reported in the literature in which high-quality SBA-15 silica was obtained with the F/Si ≤ 0.05.[37]

Diffuse-reflectance UV−vis spectroscopy is a sensitive tool that is widely used to detect the presence of framework and extraframework titanium species. Two characteristic bands have been resolved for Ti-containing materials in the UV−vis spectrum. A band with a maximum at about 200−220 nm is attributed to a ligand-to-metal charge-transfer transition in isolated TiO_4 or $HOTiO_3$ units.[38] It is generally believed to connect directly with the framework Ti^{4+} in tetrahedral coordination and is usually used as direct proof that titanium atoms have been incorporated into the framework of a molecular sieve.[38] A distinct example is the TS-1 class of molecular sieves, which generally possesses a narrow absorption band at 210 nm.[39] Another band centered at about 330 nm is typical of ligand-to-metal charge transfer occurring in bulk titania.

Figure 2 displays the UV−vis spectra of Ti−SBA-15 samples prepared with different fluoride content. They all show a very strong absorption band centered at 210 nm with a broader width than that of TS-1.[39] A broad band at 220 nm is generally observed for Ti-substituted MCM-41 materials.[13] The red-shift and increase in the width of this band have been attributed to a distorted tetrahedral coordination environment or the existence of some titanium species in an octahedral coordination environment.[40] In the present experiments, this band shows no red shift but does have a broader width. Therefore, we favor the conclusion that a part of or most of the titanium sites are in a distorted tetrahedral environment, which may be a direct consequence of the amorphous characteristics of the pore walls of the ordered mesoporous materials.[14]

For Ti−SBA-15 samples synthesized at lower fluoride content (F/Si ≤ 0.02), a shoulder at 300 nm with a tail to about 350 nm was observed. This band is believed to arise from a blue shift of bulk TiO_2 (anatase) due to quantum size effects.[41] Therefore, some TiO_2 particles or clusters may have been formed with F/Si ≤ 0.02. In contrast, UV−vis spectra of the Ti−SBA-15 samples prepared with higher fluoride content (F/Si ≥ 0.03) show no shoulder peaks at high wavelengths, which suggests that the higher content of fluoride favors the incorporation of titanium ions into the siliceous frameworks of SBA-15 materials.

The fluoride content is the only factor that differs in the synthesis process in the present experiment. Hence, the amount of fluoride used is an essential factor in determining the quality of the Ti−SBA-15 materials. In fact, the time required for the mixture of TMOS and $Ti(iOPr)_4$ to produce a white gel is shortened with an increase in the fluoride content. For example, without fluoride, the time required is about 230 min, whereas it is only about 12 min for the F/Si = 0.02 sample. Only 5 min is required for the samples at F/Si ≥ 0.03 to produce a white gel. We believe that the effect of fluoride on the incorporation of titanium ions into the siliceous frameworks of SBA-15 materials is achieved by greatly accelerating the hydrolysis rate of the TMOS. The faster the rate, the easier the formation of a Ti−O−Si bond becomes. These results suggest that the existence of fluoride is very important for the formation of Ti−SBA-15 materials. However, the amount of fluoride should be in the proper range (F/Si = 0.03−0.05) to obtain high-quality Ti−SBA-15 materials, as is the case in the synthesis of purely siliceous SBA-15 materials.[37]

B. Optimization of pH Values. The pH values are equal to that of HCl aqueous solution before the surfactant P123 was dissolved. It should be noted that the pH value increases somewhat because of the protonation[15,42] of the P123 in dilute HCl solution. For example, when P123 was dissolved in HCl solution at pH 1.0, the pH value of the final solution was about 1.5. In this series of experiments, the HCl concentration was the only variable. Other synthetic conditions, including the reaction temperature (at 60 °C), Ti content (Ti/Si = 0.01), and NH_4F content (F/Si = 0.03), were kept constant.

Figure 3 shows the XRD patterns of the Ti−SBA-15 samples prepared at different pH values. All samples show a very strong peak in the low-angle range, indicating that these samples possess periodic structures. However, the (110) and (200) peaks belonging to SBA-15-type materials are clearly resolved only for the samples prepared at pH ≤ 2.0. Only one broad peak in this range is observed for the samples prepared at pH values greater than 2.0. These results indicate that

(37) Schmidt-Winkel, P.; Lukens, W. W., Jr.; Yang, P.; Margolese, D. I.; Lettow, J. S.; Ying, J. Y.; Stucky, G. D. *Chem. Mater.* **2000**, *12*, 686.
(38) Vayssilov, G. N. *Catal. Rev.−Sci. Eng.* **1997**, *39*, 209.
(39) Petrini, G.; Cesana, A.; De Alberti, G.; Genoni, F.; Leofanti, G.; Padovan, M.; Paparatto, G.; Roffia, P. *Stud. Surf. Sci. Catal.* **1991**, *68*, 761.
(40) Blasco, T.; Corma, A.; Navarro, M. T.; Pariente, J. P. *J. Catal.* **1995**, *156*, 65.
(41) (a) Luan, Z.; Kevan, L. *J. Phys. Chem. B* **1997**, *101*, 2020. (b) Deo, G.; Turek, A. M.; Wachs, I. E.; Huybrechts, D. R. C.; Jacobs, P. A. *Zeolites* **1993**, *13*, 365.
(42) Impéror-Clerc, M.; Davidson, P.; Davidson, A. *J. Am. Chem. Soc.* **2000**, *122*, 11925.

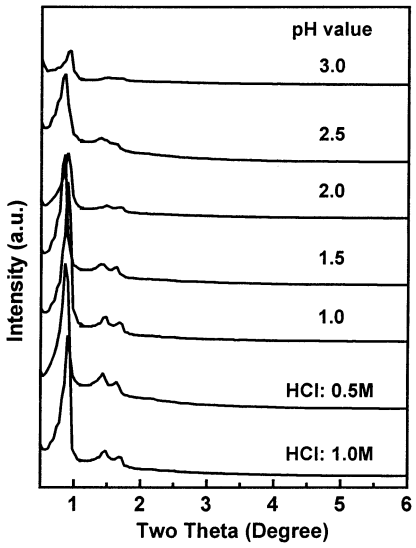

Figure 3. XRD patterns of Ti−SBA-15 samples synthesized at different pH values.

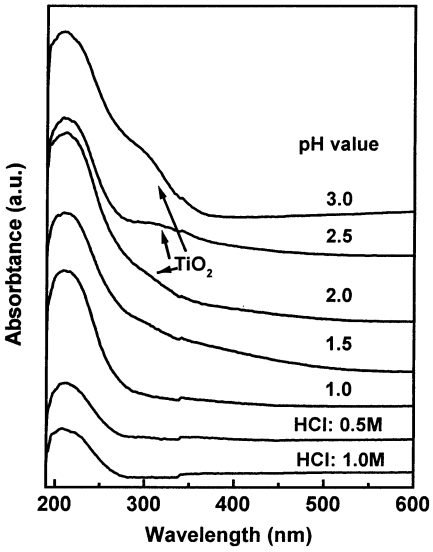

Figure 4. UV−vis absorption spectra of Ti−SBA-15 samples synthesized at different pH values.

Ti−SBA-15 materials with highly ordered structures can be obtained only under more strongly acidic conditions (pH ≤ 2.0), which is consistent with the fact that SBA-15 materials of high quality should be prepared under strongly acidic conditions.[15] In fact, high-quality SBA-15 materials are generally prepared in 1.6 M HCl solution with hydrothermal treatment at 100 °C. We have tried to synthesize Ti−SBA-15 materials directly under such conditions, but no framework titanium has been detected, although the resulting materials show highly ordered structures (analysis based on XRD and UV−vis spectrum, not shown). The reason is that Ti−O−Si bonds may be dissociated even if they have been formed under such conditions.

Figure 4 gives the UV−vis spectra of these Ti−SBA-15 samples. One strong absorption band centered at 210 nm is observed for all samples. This band indicates that titanium ions, at least in part, have been incorporated into the framework of SBA-15 materials. However, the difference in the UV−vis spectra is obvious. The samples

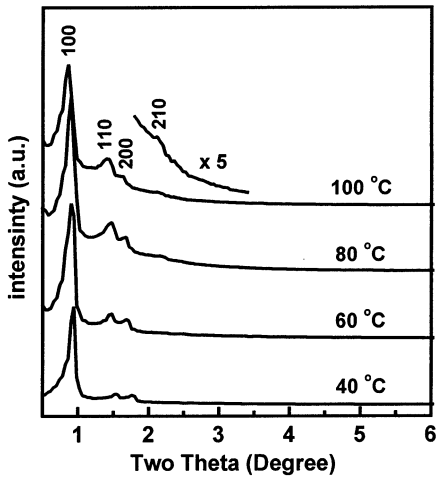

Figure 5. XRD patterns of Ti−SBA-15 samples synthesized at different temperatures.

prepared at pH ≤1.0 show only the band at 210 nm, whereas a broad tail absorption extending to 380 nm together with the band at 210 nm is detected for Ti−SBA-15 prepared at pH ≥1.5. These results suggest that bulk TiO_2 or clusters are formed in the samples prepared at pH ≥1.5.

C. Optimization of Aging Temperature. Mesoporous materials with highly periodic structures, including MCM-41, MCM-48, and SBA-15, are usually synthesized under hydrothermal conditions at temperatures higher than 100 °C. Because MCM-related materials are usually prepared under basic conditions, which have less effect on the metal−O−Si bond, the synthesis of metal-substituted MCM-related materials has been widely reported.[5] However, high-quality SBA-15 materials are generally synthesized under strongly acidic conditions through hydrothermal treatment at 100 °C, and the metal−O−Si bonds are easier to dissociate under such conditions. Therefore, the effect of the aging temperature on the quality of Ti−SBA-15 materials has been investigated in the present experiment. The Ti−SBA-15 samples were aged at 40, 60, 80, and 100 °C. Other synthetic conditions, such as F/Si = 0.03, Ti/Si = 0.01, and pH = 1.0, were constant.

The effect of the aging temperature on the periodic structures is illustrated by the XRD patterns, which are shown in Figure 5. Three typical diffraction peaks of SBA-15-type materials in low-angle ranges are observed, so all samples possess highly periodic structures. With the increase of temperature from 40 to 80 °C, the three typical peaks of SBA-15 become more clearly resolved. The Ti−SBA-15 sample prepared at 100 °C shows the fourth peak of SBA-15 materials, indexed as a (210) reflection in the patterns. These results suggest that a higher aging temperature is beneficial to the formation of SBA-15 materials with highly periodic structures. A distinct characteristic of the Ti−SBA-15 sample prepared at 100 °C is that the relative intensities of the (110) and (200) peaks are larger than those of others that were aged at lower temperatures. Such a change in the relative intensities of (110) and (200) has been discussed in the literature for MCM-41[43] and SBA-15.[44] It was shown that the samples with thicker pore walls exhibit stronger relative intensities of the (200)

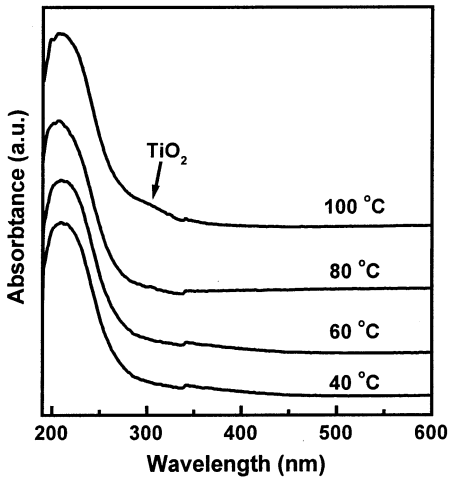

Figure 6. UV−vis absorption spectra of Ti−SBA-15 samples synthesized at different temperatures.

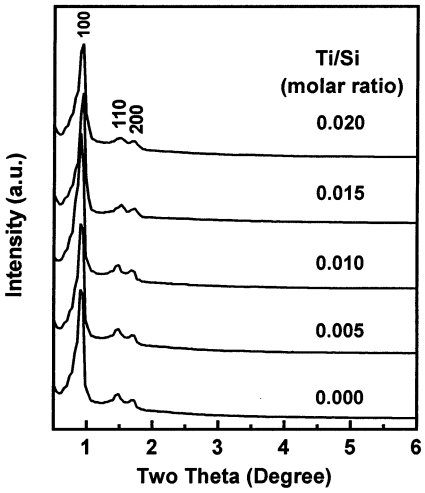

Figure 7. XRD patterns of Ti−SBA-15 samples with different titanium contents.

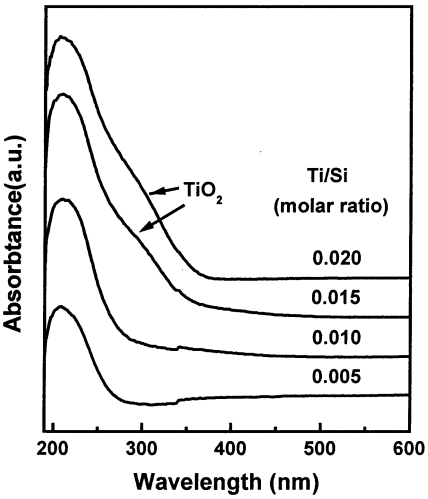

Figure 8. UV−vis absorption spectra of Ti−SBA-15 samples with different titanium contents.

peak. Impéror-Clerc et al.[42] presented another model indicating that hydrothermal treatment can improve the densities of microporous corona of SBA-15-based materials after calcination, thus giving a large intensity ratio of (110)/(200). In contrast, an inversion result was obtained for samples without hydrothermal treatment. Lindén et al.[45] reported that more complete condensation of the wall structures favors the formation of a strong (110) peak in XRD patterns. The calcined SBA-15 samples prepared at low temperatures (≤80 °C) exhibit a strong (200) peak, but it is much weaker for the samples prepared at higher temperatures (100 °C) in the present experiments. The reason should be related to all of the factors reported in these references.[42−45] It is well-known that higher hydrothermal treatment is beneficial to the complete condensation of the pore walls and induces the formation of thinner pore walls in comparison with the walls of those samples aged at lower temperatures for ordered mesoprous materials. Consequently, a relatively weak intensity of the (200) reflection peak was obtained for the sample that was hydrothermally treated at 100 °C in the present experiment.

The UV−vis spectra of these samples are shown in Figure 6. All samples possess the band at 210 nm, but only the Ti−SBA-15 sample prepared at 100 °C shows a small shoulder band at about 300 nm. These results suggest that most of the titanium ions have been incorporated into the framework of SAB-15 materials for all samples except for the sample prepared at 100 °C, which possesses some extraframework TiO_2 bulk and clusters. This TiO_2 can be explained in terms of the possible dissociation of Ti−O−Si bonds at 100 °C. As a result, extraframework titanium species are formed together with the framework titanium species. These results tell us that higher aging temperatures under acidic conditions are not suitable to the synthesis of metal-substituted mesoporous materials such as Ti−SBA-15.

D. Optimization of the Titanium Content. The experiments described above show that high-quality Ti−SBA-15 materials can be obtained with F/Si = 0.03−0.05, pH ≤ 1.0, and aging temperatures ≤80 °C. To further investigate the synthesis conditions of Ti−SBA-15 materials, samples with different titanium contents were synthesized. The Ti/Si mole ratios of the initial gel are 0.000, 0.005, 0.010, 0.015, and 0.020, respectively. Other conditions such as F/Si = 0.03, aging temperature = 60 °C, and pH 1.0 are kept constant. XRD patterns, XRF spectra, N_2 adsorption−desorption isotherms, UV−vis, UV−Raman, and ^{29}Si MAS NMR spectra, and the epoxidation reaction of styrene were used to characterize these samples.

The XRD patterns of the calcined Ti−SBA-15 samples with various titanium contents are present in Figure 7. All samples show the characteristic patterns of SBA-15 materials, meaning that high-quality SBA-15-type materials are synthesized.

The UV−vis spectra of these samples are shown in Figure 8. The absorption band at about 210 nm is observed for all samples, meaning that titanium ions have been incorporated into the frameworks of SBA-15

(43) (a) Feuston, B. P.; Higgins, J. B. *J. Phys. Chem.* **1994**, *98*, 4459. (b) Kruk, M.; Jaroniec, M.; Sayari, A. *Chem. Mater.* **1999**, *11*, 492. (c) Ågren, P.; Lindén, M.; Rosenholm, J. B.; Schwarzenbacher, R.; Kriechbaum, M.; Amenisch, H.; Laggner, P.; Blanchard, J.; Schüth, F. *J. Phys. Chem. B* **1999**, *103*, 5943.

(44) Kruk, M.; Jaroniec, M.; Ko, C. H.; Ryoo, R. *Chem. Mater.* **2000**, *12*, 1961.

(45) Lindén, M.; Blanchard, J.; Schacht, S.; Schunk, S. A.; Schüth, F. *Chem. Mater.* **1999**, *11*, 3002.

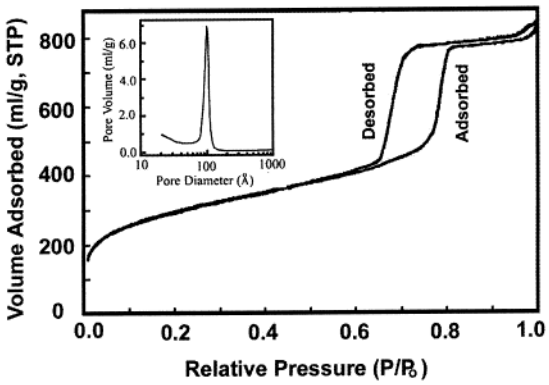

Figure 9. Nitrogen adsorption−desorption isotherm of a Ti−SBA-15 sample with Ti/Si = 0.010 in the initial gel.

materials in the present experiments. The intensity of this band is found to increase monotonically with the increase of Ti/Si ratios from 0.000 to 0.015 and to remain unchanged with a further increase from 0.015 to 0.020. It should be noted that the shoulder peak centered at about 300 nm with a tail to about 350 nm was observed for the two Ti−SBA-15 samples with Ti/Si = 0.015 and 0.020, suggesting that extraframework TiO_2 particles were formed in them. These results may reflect the trend that the framework titanium content increases with the titanium content in the starting gels. The maximum content in the initial gel should be less than 0.015 to obtain high-quality Ti−SBA-15 materials.

The porosity of the Ti−SBA-15 samples has been measured by N_2 sorption analysis. Figure 9 gives the adsorption−desorption isotherm and pore-size distribution of the Ti−SBA-15 sample with Ti/Si = 0.010. The isotherm is of type IV and shows steep hysteresis of type H1 at high relative pressure, which is typical of mesoporous materials that have large pore sizes with narrow size distributions.[46] However, the isotherm of the Ti−SBA-15 samples in the present experiment is different from those of siliceous SBA-15 materials in the literature[15] in that an obvious hysteresis of the H3 type at $P/P_0 \geq 0.8$ is observed. This is an indication of N_2 condensation and evaporation within interparticles[46] or of some impurity phase, such as lamellar mesostructures that are sometimes generated by liquid-crystal-templated materials.[47]

Figure 10 shows the ^{29}Si MAS NMR spectra for the series of as-synthesized Ti−SBAS-15 samples. Three bands centered at −93, −103, and −113 ppm are resolved, and these bands can be attributed to $Si(OSi)_x(OH)_{4-x}$ framework units where $x = 2$ (Q^2), $x = 3$ (Q^3), and $x = 4$ (Q^4).[48] The relatively strong intensities of the Q^2 and Q^3 bands show that there are a large number of silanol groups in these samples. The intensity of Q^3 gradually decreases when the titanium content increases from Ti/Si = 0.000 to 0.010 in the gels. However, a further increase in the titanium content from 0.010 to 0.020 results in no appreciable change in the intensity of the Q^3 band. These results suggest that titanium incorporation promotes cross linking of the

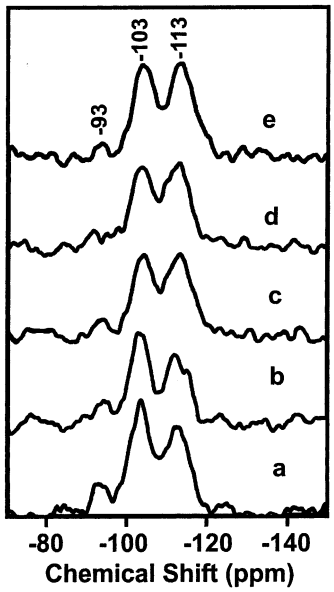

Figure 10. ^{29}Si MAS NMR spectra of Ti−SBA-15 samples with different titanium contents. (a) Si−SBA-15, (b) Ti−SBA-15 (Ti/Si = 0.005), (c) Ti−SBA-15 (Ti/Si = 0.010), (d) Ti−SBA-15 (Ti/Si = 0.015), and (e) Ti−SBA-15 (Ti/Si = 0.020) Note that the value of Ti/Si is that of the initial gels.

frameworks of Ti−SBA-15. Similar results have been reported for metal-substituted MCM-41 systems.[14,49] These results also suggest that the maximum amount of incorporated titanium is about 0.010 (Ti/Si) in the starting gel, consistent with the results of UV−vis spectra. However, elemental analysis by XRF spectroscopy showed that the titanium content of the products is much less than that of the initial gels, which is possibly due to a portion of the Ti that remains in the acidic solution. The corresponding data of Ti content are given in Table 1. A similar result has been reported for Ti-MCM-41 prepared under acidic conditions.[14]

UV−Raman spectroscopy has been demonstrated to be a powerful technique for the identification of incorporated framework transition-metal ions in metal-containing zeolites[50] and MCM-41 materials.[51] UV−Raman spectroscopy has no fluorescence background for which to correct, thus greatly improving its sensitivity. Furthermore, the resonance Raman effect can selectively enhance the Raman bands that are directly associated with the framework metal while keeping the remaining Raman bands unchanged for metal-containing molecular sieves. In this work, the charge-transfer ($O^{2-} \rightarrow Ti^{4+}$) absorption band is centered at 210 nm; therefore, UV−Raman spectroscopy can be used to identify the states of titanium species on the basis of resonance Raman effects. Figure 11 displays the UV−Raman spectra of Ti−SBA-15 samples with different titanium contents. For the purely siliceous sample (Si−SBA-15), three Raman bands at 489, 789, and 966

(46) Gregg, S. J.; Sing, K. S. W. *Adsorption, Surface Area, and Porosity*; Academic Press: London, 1982.
(47) Huo, Q.; Leon, R.; Petroff, P. M.; Stucky, G. D. *Science (Washington, D.C.)* **1995**, *268*, 1324.
(48) Sindorf, D. W.; Maciel, G. E. *J. Am. Chem. Soc.* **1981**, *103*, 4263.
(49) (a) Chatterjee, M.; Iwasaki, T.; Hayashi, H.; Onodera, Y.; Ebina, T.; Nagase, T. *Chem. Mater.* **1999**, *11*, 1368. (b) Alba, M. D.; Luan, Z.; Klinowski, J. *J. Phys. Chem.* **1996**, *100*, 2178.
(50) (a) Li, C.; Xiong, G.; Xin, Q.; Liu, J. K.; Ying, P. L.; Feng, Z.; Li, J.; Yang, W. B.; Wang, Y. Z.; Wang, G. R.; Liu, X. Y.; Lin, M.; Wang, X. Q.; Min, E. Z. *Angew. Chem., Int. Ed.* **1999**, *38*, 2220. (b) Yang, Q.; Wang, S.; Lu, J.; Xiong, G.; Li, C. *Appl. Catal., A* **2000**, *194*, 507. (c) Li, C.; Xiong, G.; Liu, J.; Ying, P.; Xin, Q.; Feng, Z. *J. Phys. Chem. B* **2001**, *105*, 2993.
(51) Xiong, G.; Li, C.; Xin, Q.; Feng, Z. *Chem. Commun.* **2000**, 677.

Table 1. Texture Properties and Selective Oxidation of Styrene for Ti−SBA-15 Samples with Different Titanium Contents

sample	Ti/Si (initial gel) (mol %)	Ti/Si (final product) (mol %)	BET surface area (m^2/g)	pore diameter (nm)	pore volume (mL/g)	conversion of styrene (mol %)[a]	selectivity (mol %)	
							benzaldehyde	epoxide
1			968.2	9.58	1.177			
2	0.5	0.10	968.1	9.74	1.193	9.9	55.2	44.8
3	1.0	0.21	1040.9	9.81	1.169	19.3	51.2	48.8
4	1.5	0.43	1044.5	9.75	1.157	38.2	50.3	49.7
5	2.0	0.56	1009.5	9.64	1.057	37.2	52.7	47.3

[a] Conversion (mol %) = (converted styrene/H_2O_2) × 100.

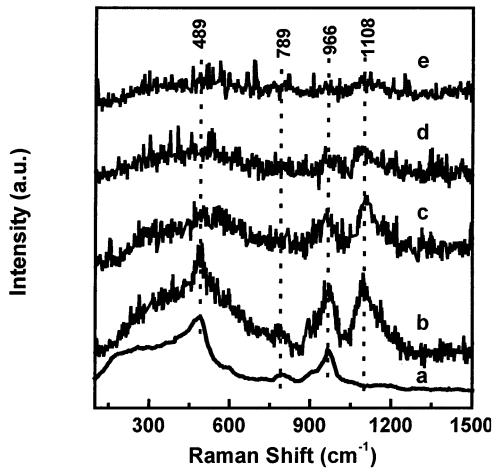

Figure 11. UV−Raman spectra of Ti−SBA-15 samples with different titanium contents. (a) Si−SBA-15, (b) Ti−SBA-15 (Ti/Si = 0.005), (c) Ti−SBA-15 (Ti/Si = 0.010), (d) Ti−SBA-15 (Ti/Si = 0.015), and (e) Ti−SBA-15 (Ti/Si = 0.020) Note that (a) the value of Ti/Si is that of the initial gels and (b) the intensities of the UV−Raman signals of all of the Ti−SBA-15 samples have been magnified 10 times.

cm^{-1} are observed. The first band is assigned to the asymmetric stretching vibration of the Si−O−Si bond; the second one is associated with the symmetric stretching mode of the Si−O−Si bond;[52] and the last one is associated with the Si−O−Si bond that is directly related to the framework defects, such as surface silanol groups.[51a,c,52] For the Ti−SBA-15 samples, the UV−Raman spectra clearly show a new, strong band at 1108 cm^{-1}, which arises from the resonance Raman effects of the framework titanium species and should be assigned to the asymmetric stretching vibrations of the Ti−O−Si bonds of the framework titanium species.[50a,c,51b] A noteworthy trend is that all band intensities decrease with increasing titanium content. Considering the results of the UV−vis spectra, this trend may be attributed to the amount of change on the extraframework titanium species. For Ti−SBA-15 samples with Ti/Si = 0.005 and 0.010, the titanium ions should be located mainly in the framework in an isolated state, whereas there are some titanium species existing in an extraframework state in the Ti−SBA-15 samples with higher titanium contents. These extraframework titanium species absorb the UV−Raman scattering, thus diminishing the Raman signal intensity. Therefore, a higher signal-to-noise ratio is obtained only when Ti/Si ≤ 0.010.

It is noteworthy that the intensities of the Raman signals for all Ti−SBA-15 samples have been magnified 10 times, so the signal-to-noise ratios for all Ti-containing samples are relatively poor compared with that of the purely siliceous sample. The explanation is similar to that given in the above discussion, namely, there is a small number of extraframework titanium species in all of the titanium-containing samples, although the band of TiO_2 is not seen in the UV−vis spectra for Ti−SBA-15 samples of lower titanium content (Ti/Si ≤ 0.010).

The catalytic results for the epoxidation of styrene on Ti−SBA-15 with different contents of titanium are presented in Table 1. All of the samples show considerable activity, and the styrene conversion and epoxidation selectivity depend strongly on the Ti content in the Ti−SBA-15 materials. For example, sample 4 has a styrene conversion of 38.2% and an epoxidation selectivity of 49.7%. These data are appreciatively higher than those of Ti-MCM-41 prepared under acidic conditions[14] but are somewhat lower than those of Ti−SiO_2 prepared by ion beam implantation.[53] One possible reason is that SBA-15 materials possess larger pores than do MCM-41 and also smaller pores across their pore walls.[26b] These smaller pores may be very beneficial to the diffusion of styrene molecules in the pores of SBA-15 so that Ti−SBA-15 shows a higher activity than does Ti-MCM-41. On the basis of the above characterization, we expect the highest framework titanium content to be found in sample 4 or 5. This expectation is in accordance with the conclusion that the framework Ti is the active center for the epoxidation of olefins.[14,53]

Conclusions

Ti-substituted SBA-15 materials have been successfully synthesized by a direct synthesis method through the fluoride-accelerating hydrolysis of TMOS and have been characterized by bulk and microanalytic techniques. The optimization of fluoride content, the pH value of the HCl solution, the aging temperature, and the relationship of the content of titanium in the starting gels to the quality of the resulting Ti−SBA-15 materials have been systematically investigated. The results show that Ti−SBA-15 samples can be synthesized under conditions of F/Si > 0.03, Ti/Si < 0.01, pH < 1.0, and aging temperatures < 80 °C. These materials show relatively high activity and selectivity in the epoxidation of styrene. We found that there is no stoichiometric incorporation of Ti, that the achieved Ti content is quite low for the proposed approach, and that fluoride plays an essential role in the formation of Ti−SBA-15 materials of high quality. Fluoride can

(52) Brinker, C. J.; Kirkpatrick, R. J.; Tallant, D. R.; Bunker, B. C.; Montez, B. *J. Non-Cryst. Solids* **1988**, *99*, 418.
(53) Yang, Q.; Li, C.; Yuan, S.; Li, J.; Ying, P.; Xin, Q.; Shi, W. *J. Catal.* **1999**, *183*, 128.

significantly enhance the hydrolysis rate of TMOS to better match the hydrolysis rate of the titanium precursors. As a result, titanium ions can be more efficiently incorporated into the siliceous framework.

Acknowledgment. This work was granted financial support from the China Postdoctoral Science Foundation for W.-H.Z. and was supported by the Natural Science Foundation of China (NSFC grant no. 20073045). W.-H. Z. is grateful to Mr. Steven Zhang at the Shanghai Branch, BASF (China) Company Limited, for supplying the P123 surfactant.

CM011686C